16th European Signal Processing Conference (EUSIPCO 2008), Lausanne, Switzerland, August 25-29, 2008, copyright by EURASIP

NONLINEAR SET MEMBERSHIP TIME SERIES PREDICTION OF BREATHING

Guy Tchoupo and Alen Docef

Department of Electrical and Computer Engineering, Virginia Commonwealth University
601 West Main Street, 23284-3068, Richmond, USA
phone: + (1) 804-828-0181, fax: + (1) 804-828-4269, email: adocef@vcu.edu
web: www.egr.vcu.edu

ABSTRACT

In radiation therapy, tumor motion induced by patient's respiration may lead to significant differences between the planned and delivered radiation dose. Compensating for tumor motion is therefore crucial for accurate and efficient treatment. The focus of the presented research is on real-time tumor tracking, due to its potential to overcome the limitations of other approaches, such as margin expansion, breath-holding, and gating. A real challenge in tumor tracking is the presence of delays in the treatment system. Prediction of tumor displacement is then necessary to overcome such delays. In this paper, we propose a method for the prediction of breathing signals based on a Nonlinear Set Membership (NSM) algorithm. The algorithm does not require the choice of a predefined functional form for the prediction model, and addresses the issue of measurement noise with minimal assumptions on its statistical properties. The NSM method was tested on nine clinical signals and its performance compared favorably with reported results as well as an optimized nonlinear neural network predictor.

1. INTRODUCTION

Tumor motion induced by respiration represents a real challenge for the accurate delivery of conformal radiation treatment. In fact, a tumor embedded in organs that are subject to respiratory motion appears to be deformed during respiratory cycle [1]. Such deformation may result in large displacements of treatment sites from their planned position. As a result, healthy tissue may be exposed to radiation, and the actual dose distribution delivered using external-beam radiotherapy may significantly differ from the prescribed distribution. Methods for compensation of respiration-induced organ motion may be classified into four categories: (1) margin expansion [2, 3], (2) breath-holds (voluntary and forced) [4, 5], (3) gating [6, 7] and (4) real-time tracking [8, 9, 10]. Margin expansion increases the volume of exposed healthy tissue surrounding the tumor. The breath-hold approach requires the patient to hold respiration during treatment, which may be poorly tolerated by pulmonary compromised patients. Gated radiotherapy consists of synchronizing the radiation beam with the patient breathing cycle and turning the beam on only during a precise time window. This increases the treatment time. The real-time tracking approach has the potential to overcome the limitations of the above mentioned techniques. The presence of delays in the real-time tracking system (up to several hundred milliseconds) requires the capability to predict the tumor position. An estimate of the tumor position is usually obtained from the measurement of an external marker placed on the patient's chest. Therefore, an algorithm for the prediction of the breathing pattern is needed.

Due to the diversity and complexity of the breathing cycle [11, 12], the prediction algorithm must be sophisticated enough to handle a variety of possible breathing signals, [13]. The prediction problem can be summarized as follows: given a set of breathing signal measurements, y^t, $t = 1, 2, ..., T$, compute a predicted value $\hat{y}^{T+k}$ of y^{T+k}, such that the prediction error $|\hat{y}^{T+k} - y^{T+k}|$ is small. The parameter $k \geq 1$ is called the prediction horizon. The measurements y^t are assumed to be generated by a dynamic system of the form:

$$y^{t+1} = f_0(w^t) \tag{1}$$

where $w^t = [y^t, y^{t-1}, ..., y^{t-n_y+1}]$ is the regressor vector, $n_y > 0$ is the model order, and $f_0(.)$, is a function to be determined.

A conventional approach in tumor motion prediction is to employ a predefined functional form for f_0, in Equation (1). In [14], the author developed a bio-mechanical model for the breathing process. In [15], [16], and [17], simple harmonic functional forms have been considered. Such models have difficulty capturing transients and highly irregular patterns in the breathing signal. The use of linear and nonlinear filters as functional forms for f_0 has also been investigated. In [18, 19, 17], the authors concluded that adaptive filters and neural networks (NN) with coefficients updated using the Least Mean Square (LMS) algorithm performed better than the Kalman filter for non-stationary breathing signals. It was also noted that nonlinear adaptive filters outperformed linear filters for signals with a high degree of irregularity. Nonlinear NN with a single neuron [20], multiple neurons [21], and with fuzzy logic training [22] have been proposed, but have not been tested on extremely irregular breathing signals. It is therefore premature to conclude on their suitability for real life breathing behavior. In [23], an LMS algorithm and a nonlinear NN were tested on highly irregular breathing. The nonlinear NN, with weights updated using the LMS algorithm, was in general found to be more robust and have a better prediction performance than the LMS filter. In [24], the Recursive Least Square (RLS) algorithm was found to perform better than the LMS filter when applied on quasi-regular breathing signals. In addition, the LMS approach is very sensitive to the choice of the step size, which prevents it from achieving consistent performance for a wide variety of breathing signals.

All the above mentioned algorithms constrain f_0 to have a predetermined form. This constraint can limit the prediction performance, especially for large prediction horizons. In this paper we propose an alternative method, the Nonlinear Set Membership (NSM) [25], which does not assume to know the functional form of f_0, but uses some information on its regularity, given by bounds on the gradients of f_0. In addition

the measurements are assumed to be corrupted by bounded noise, in contrast with statistical methods, which rely on assumptions such as, regularity, ergodicity, uncorrelation, type of distribution, etc, [26], which validity may be difficult to be reliably tested in practice. In this paper, the NSM method is tested on nine real clinical data and its performance is compared with reported results as well as the performance of an optimized Neural Networks predictor.

This paper is organized as follows. In Section 2 the NSM algorithm is introduced. Afterwards, in Section 3, the experimental setup for NSM and NN prediction is described. Prediction performance experimental results are presented and discussed in Section 4. Concluding remarks are given in Section 5.

2. THE NSM PREDICTION ALGORITHM

As introduced in [25], the Nonlinear Set Membership (NSM) algorithm for time series prediction relies on some assumptions on the functional form f_0 defined in Equation (1), and on the noise sequence. Consider that a set of noise corrupted data $\tilde{Y}^T = [\tilde{y}^1, \tilde{y}^2, ..., \tilde{y}^T]$ and $\tilde{W}^T = [\tilde{w}^1, \tilde{w}^2, ..., \tilde{w}^T]$ generated by Equation (1) is available. Then $\tilde{y}^{t+1} = f_0(\tilde{w}^t) + d^t$ for $t = 1, 2, ..., T-1$, where the term d^t accounts for the fact that y^{t+1} and w^t are not exactly known.

The following prior assumptions are made on the function f_0 and the noise:

- f_0 is continuous and has a finite gradient:

$$f_0 \in \mathscr{K} \doteq \{f \in C^1(W) : \|\nabla f\| \leq \gamma\} \tag{2}$$

  where $W \subseteq \mathscr{R}^{n_y}$ and $\|.\|$ is the Euclidean norm. ■
- the noise components are finite:

$$D^T \in \mathscr{D} \doteq \{[d^1, d^2, ..., d^T] : |d^t| \leq \varepsilon^t + \gamma\delta^t, t = 1, 2, ..., T\} \tag{3}$$

  where ε^t is the bound on noise affecting the measurement y^t, $|y^{t+1} - \tilde{y}^{t+1}| \leq \varepsilon^t$, and δ^t is the bound on noise affecting the regressor vector w^t, $\|w^t - \tilde{w}^t\| \leq \delta^t$. ■

It is necessary to define the set of systems that are consistent with prior assumptions and measured data.

Definition 1 *The feasible system set FSS^T is*

$$FSS^T \doteq \{f \in \mathscr{K} : |\tilde{y}^{t+1} - f(\tilde{w}^t)| \leq \varepsilon^t + \gamma\delta^t, t = 1, 2, ..., T-1\} \tag{4}$$

■

The feasible set FSS^T summarizes all the information (measured data and prior assumptions on f_0 and d) that is available up to time T about the signal's dynamics. If the data validate the assumptions made on f_0 and d, then the FSS^T is said to be not empty, ($\text{FSS}^T \neq \emptyset$), and prediction can be performed using such assumptions.

In order to define the necessary and sufficient condition for the assumptions to be validated, the following functions are introduced:

$$\overline{f}(w) \doteq \min_{t=1,...,T-1} (\overline{h}^t + \gamma\|w - \tilde{w}^t\|) \tag{5a}$$

$$\underline{f}(w) \doteq \max_{t=1,...,T-1} (\underline{h}^t - \gamma\|w - \tilde{w}^t\|) \tag{5b}$$

where $\overline{h}^t \doteq \tilde{y}^{t+1} + \varepsilon^t + \gamma\delta^t$ and $\underline{h}^t \doteq \tilde{y}^{t+1} - \varepsilon^t - \gamma\delta^t$.

Theorem 1 *: [27], [25]:*

a) A necessary condition for prior assumptions to be validated is
$\overline{f}(\tilde{w}^t) \geq \underline{h}^t, \qquad t = 1, ..., T-1$

b) A sufficient condition for prior assumptions to be validated is
$\overline{f}(\tilde{w}^t) > \underline{h}^t, \qquad t = 1, ..., T-1$

■

Theorem 1 can be used to find the values of ε^t, δ^t, and γ that validate the prior assumptions. In order to simplify the algorithm, constant bounds can be considered, i.e. $\varepsilon^t = \varepsilon$ and $\delta^t = \delta$ for all values of t.

In the space $(\varepsilon, \delta, \gamma)$, the function

$$\gamma^*(\varepsilon, \delta) \doteq \inf_{\text{FSS}^T \neq \emptyset} \gamma \tag{6}$$

represents a surface that separates falsified values of ε, δ and γ from the validated ones. For the purpose of prediction, the triplet $(\varepsilon, \delta, \gamma)$ must be chosen in the validated parameters region.

Theorem 2 *: [25]: The predicted value $\hat{y}^{T+k}$ is computed as:*

$$\hat{y}^{T+k} = \frac{1}{2}[\underline{f}(\tilde{w}^T) + \overline{f}(\tilde{w}^T)]. \tag{7}$$

A detailed proof and an optimality analysis of the algorithm can be found in [25].
The NSM algorithm compares the current signal history, w^T with the previous history vector, w^t, $t = 1, ..., T-1$ stored in W^t, and finds the two closest matching vectors corresponding to the two metrics Equations (5a), and (5b). Then it computes the predicted value $\hat{y}^{T+k}$ using Equation 7.

3. THE EXPERIMENTAL SETUP

3.1 The breathing data

The breathing patterns used in this work have been collected while the patients breathed freely. The Synchrony® respiratory tracking subsystem, part of the Cyberknife® system at Georgetown University Medical Center, was used to capture the signals [23]. The patients were neither coached in breathing technique nor otherwise subjected to breathing regulation. Therefore the data can be considered a fair record of each patient's normal breathing. The signals were sampled at 30 Hz and further downsampled to 10 Hz to allow a fair comparison with results reported in [23]. We used the breathing data for nine different patients to analyze the ability of the NSM algorithm to predict respiratory signals up to 500 ms in advance. As reported in [23], these examples were selected arbitrarily (i.e., without prejudice as to how well or poorly the prediction algorithm might work) to represent a variety of breathing behaviors.

For the purpose of evaluating prediction performance, each patient's breathing data was divided into three consecutive subsets. An estimation set, I_{est}, composed of samples in the first 40 s, a calibration set, I_{cal}, formed of the samples in the following 40 s, and a validation set, I_{val}, composed of samples in the last 80 s of the signal. For each of the prediction methods, I_{est} is used to train or design the predictor, I_{cal} for its calibration, and finally I_{val} is used to measure its prediction performance. The above time interval subdivision

is adopted to allow a fair comparison with reported results, [23]. The prediction performance is measured using the Normalized Root Mean Square Error (NRMSE), computed as $NRMSE = \sqrt{\frac{\sum_{t=1}^{N}(y^{k+t}-\hat{y}^{k+t})^2}{\sum_{t=1}^{N}(y^{k+t}-\overline{Y})^2}}$, where N is the total number of predicted samples, $\overline{Y}$ the arithmetic mean of y^t.

3.2 The NSM prediction procedure

During the NSM prediction procedure, for simplicity, the measurement devices are assumed to be perfect, i.e. $\varepsilon^t = 0$ for all t, and in addition it is supposed that $\delta^t = \delta$, for all t. The NSM prediction experiment consists of three parts: estimation, calibration and validation. In the *estimation phase*, the assumptions, Equation (2) and Equation (3) are validated through verification of the condition defined in Theorem 1b. The separation curve, $\gamma^*(\delta)$ defined in Equation (6), separating the falsified region form the validated one, is computed, using the estimation data, $\mathrm{I_{est}}$. In the *calibration phase* prediction performance is computed using the calibration data, $\mathrm{I_{cal}}$, using Equation (7) for each pair (γ, δ) in the validated region. At the end of this phase the pair $(\hat{\gamma}, \hat{\delta})$ with smallest prediction error on $\mathrm{I_{cal}}$ is chosen to be used during the final phase. During the *validation phase*, NSM prediction is performed on the validation data, $\mathrm{I_{val}}$, using $(\hat{\gamma}, \hat{\delta})$ in Equation (7) and the corresponding prediction performance is evaluated. This last phase corresponds to the prediction algorithm used during the actual treatment.

3.3 The Neural Networks prediction procedure

In this work we tested a feed-forward backpropagation NN composed of one input layer with n_y neurons, a hidden layer with 2 neurons, and an output layer with 1 neuron. A sigmoid activation function of the form, $f(x) = 1/(1+e^{-x})$ is used to transfer information form the hidden layer to the output layer. A simple identity function $(f(x) = x)$ is used to connect the output layer neurons to the network's output. Each NN weight is updated using the Least Mean Square (LMS) algorithm, $B_{t+1} = B_t + \mu e^t w^t$, where $e^t = \hat{y}^{t+k} - y^{t+k}$ is the current prediction error and μ is the update step size. The network uses the well-known Widrow-Hoff learning approach, and the Levenberg-Marquardt algorithm is used as a training method.

To avoid the situation where the NN prediction performance is dependent on the network initialization, all the weights are initialized with fixed values. Thus, before network training, the three biases are initialized with zero values, the weight matrix connecting the input layer to the hidden layer is set to a$(n_y \times 2)$ matrix formed of ones in the first row and zeros for the remaining $(n_y - 1)$ rows, and the weights connecting the hidden layer to the output layer are all set to one.

The predictor is optimized by training the NN for a number of epochs ranging form 1 to 50, with $\mu \in [10^{-5}, 2]$, and a step size of 10^{-5} using the estimation data, $\mathrm{I_{est}}$. After each training, the NN predictor performance is evaluated using the calibration data, $\mathrm{I_{cal}}$. We then chose the best NN predictor,(i.e. with smallest prediction error on the calibration set), and its performance is then evaluated by performing prediction using the validation set, $\mathrm{I_{val}}$. Using a number of epochs greater than 50 resulted in overtraining.

4. RESULTS AND DISCUSSION

A key parameter of the prediction algorithm is the choice of the regressor's size, n_y. In fact, this parameter determines the number of samples in the past that are to be used to predict future samples. Several regressor sizes ranging from 1 to 30 have been tried, and a value of $n_y = 25$ appeared to give the best average prediction performance in term of NRMSE for the nine breathing signals and for both the NSM and NN approaches. The prediction performance of the NSM algorithm is presented here and compared to the optimized NN algorithm and to the results reported in [23]. The latency is varied from 100 ms to up to 500 ms. Plots of three examples of NSM prediction performance, for a 300 ms prediction, are also presented.

- **I** In Figure 2(a) the original and predicted breathing signals of patient 1 for a 300 ms latency are shown, and the corresponding prediction error is presented in 2(b). The separation curve, the chosen parameter γ, δ and corresponding NRMSE (when prediction is performed on $\mathrm{I_{cal}}$) can be seen in Figure 1. This signal features a long, complicated transient interrupting regular breathing. Both the NSM and optimized NN performed better than the simple NN [23], but for latencies greater than 200 ms, the NSM predictor performs better than the optimized NN.
- **II** The original and predicted breathing signal, and corresponding prediction error for patient 2 are presented in Figure 3(a) and 3(b), respectively. This signal corresponds to regular breathing with a slightly time-varying period. Here the optimized NN performs better than both the regular NN and the NSM. As the latency increases, the performances of the NSM and the optimized NN become similar.
- **III** The signals for patient 3 are presented in Figure 4(a) and the corresponding prediction error is shown in Figure 4(b). This signal corresponds to highly irregular breathing that is difficult to predict using a simple NN. The NSM appears to perform better than the optimized NN, as well as the normal NN.

A summary of the prediction performance for the three prediction algorithms is presented in Table 1, for latencies up to 500 ms. In general, the NSM performed better than the optimized NN as well as the NN proposed in [23].

5. CONCLUSION

In this paper, an NSM algorithm was used to predict regular and irregular breathing. Compared to existing approaches, this method does not rely of the assumption of a predefined functional form for the model used for prediction, which can limit prediction performance, especially for large latencies. The NSM method has been applied to nine real clinical signals. The method compares favorably with other reported results, for a wide variety of breathing scenarios, at least for latencies up to 500 ms. Due to its robustness, the NSM method is a valid approach to consider when attempting real-time tumor motion compensation.

Acknowledgment

We would like to thank Dr. Martin J. Murphy of the Department of Radiation Oncology at Virginia Commonwealth University for providing us with the data and for fruitful discussion.

REFERENCES

[1] S. S. Vedam, P. J. Keall, V. R. Kini, H. Mostafavi, H. P. Shukla, and R. Mohan. Acquiring a four-dimensional computed tomography dataset using an external respiratory signal. *Phys. Med. Biol.*, 48:42–62, 2003.

[2] Valdani, R., C. Italia, P. Montanaro, M. Ciocca, G. Morandi, and B. Salvadori. Clinical target volume localization using conventional methods (anatomy and palpation) and ultrasonography in early breast cancer post-operative external irradiation. *Radiother. Oncol.*, 3(231-237), 1997.

[3] Van de Steene, J. N. Linthou, J. de Mey, V. Vinh-Hung, C. Claassens, M. Noppen, A. Bel, and G. Storme. Definition of gross tumor volume in lung cancer: Inter-observer variability. *Radiother. Oncol.*, 62(1):37–49, 2002.

[4] J. Hanley et al. Deep inspiration breath-hold technique for lung tumors: The potential value of target immobilization and reduced lung density in dose escalation. *Int. J. Radiat. Oncol. Biol. Phys.*, 45:603–611, 1999.

[5] K. E. Rosenzweig et al. The deep inspiration breath-hold technique in the treatment of inoperable non-small-cell lung cancer. *Int. J. Radiat. Oncol. Biol. Phys.*, 48:81–87, 2000.

[6] G. Hugo, N. Agazaryan, and T. D. Solberg. The effects of motion on planning and delivery of respiratory-gated IMRT. *Med. Phys.*, 30:1052–1066, 2003.

[7] S. S. Vedam, P. J. Keall, V. R. Kini, and R. Mohan. Determining parameters for respiration-gated radiotherapy. *Med. Phys.*, 228:2139–2146, 2000.

[8] P. J. Keall, V. R. Kini, S. S. Vedam, and R. Mohan. Motion adaptive x-ray therapy: A feasibility study. *Phys. Med. Biol.*, (46):1–10, 2001.

[9] M. J. Murphy. Tracking moving organs in real time. *Semin. Radiat. Oncol.*, 14:91–100, 2004.

[10] W. D. D'Souza, S. A. Naqvi, and C. X. Yu. Real time intra-fraction motion tracking using the treatment couch; a feasibility study. *Phys. Med. Biol.*, 50:4021–4033, December 2005.

[11] G. Benchetrit. Breathing pattern in humans: Diversity and individuality. *Resp. Phisiol.*, pages 122:123–129, 2000.

[12] P. Liang, J. J. Pandit, and P. A. Robbins. *Modeling and Control of Ventilation*, chapter Non-sationary of breath-by-breath ventilation and Approaches to Modling the Phenomenon, pages 117–121. New York Pleanum NY, 1995.

[13] G. C. Donaldson. The chaotic behaviour of resting human respiration. *Resp. Phisiol.*, pages 313–321, 1992.

[14] D. A. Low, P. J. Parikh, J. F. Dempsey, S. H. Wahab, J. P. Hubenschmidt, M. M. Nystrom, M. Handoko, and J. D. Bradley. A novel breathing motion for radiation therapy. *Int. J. Radiat. Oncol. Phys.*, (63):921–9, 2005.

[15] Y. Seppenwoodle, H. Shirato, S. Shimizu, M. van Herk, J. V. Lesbeque, and K. Miyasaka. Precise real-time measurement of 3d tumor motion in lung due to breathing and heartbeat measured during radiotherapy. *Int. J. Radiat. Oncol. Biol. Phys.*, 53:822–834, 2002.

[16] T. Neicu, H. Shirato, and Y. Seppenwoolde. Synchonized moving aperture radiation therapy (SMART): Average tumor trajectory for lung patients. *Phys. Med. Biol.*, (48):587–598, 2003.

[17] S. S. Vedam, P. J. Keall, A. Docef, D. A. Todor, V. R. Kini, and R. Mohan. Predicting respiratory motion for four-dimensional radiotherapy. *Med. Phys.*, 31(8):2274–2283, August 2004.

[18] M. J. Murphy, J. Jalden, and M. Isakson. Adaptive filtering to predict lung tumor breathing motion during image-guided radiation therapy. In 16^{th} *International Congress on Computer-assisted Radiology and Surgery*, 2002.

[19] M. Isacksson, J. Jalden, and M. J. Murphy. On using an adaptive neural network to predict lung tumor motion during respiration radiotherapy applications. *Med. Phys.*, 32(12):3801–3809, December 2005.

[20] H. Yan, F. Yin, G. Zhu, M. Ajlouni, and J. H. Kim. Adaptive prediction of internal target motion using external motion: a technical study. *Phys. Med. Biol.*, 51:31–44, 2006.

[21] G. C. Scharp, S. B. Jiang, S. Shimizu, and H. Shirato. Prediction of respiratory tumor motion for real-time image-guided radiotherapy. *Phys. Med. Biol.*, 49:425–440, 2004.

[22] M. Kakar, H. Nystrom, L. R aarup, T. J. Nottrup, and D. R. Olsen. Respiratory motion prediction by using the adaptive neuro fuzzy inference system. *Phys. Med. Biol.*, (50):4721–8, 2005.

[23] M. J. Murphy and S. Dieterich. Comparative performance of linear and nonlinear neural networks to predict irregular breathing. *Phys. Med. Biol.*, (51):5903–5914, 2006.

[24] P. Qiu, W. D. D'Souza, T. J. Mc Avoy, and K. J. Ray Liu. Inferential modeling and predictive feedback control in real-time motion compensation using the treatment couch during radiotherapy. *Phys. Med. Biol.*, (52):5831–5854, 2007.

[25] M. Milanese and C. Novara. Set membership prediction of nonlinear time series. *IEEE Transactions on Automatic Control*, 50(11):1655–1669, November 2005.

[26] L. Ljung. *System Identification: Theory for User*. Prentice Hall, second, 1999.

[27] M. Milanese and C. Novara. Set membership identification of nonlinear systems. *Automatica*, 40:957–975, 2004.

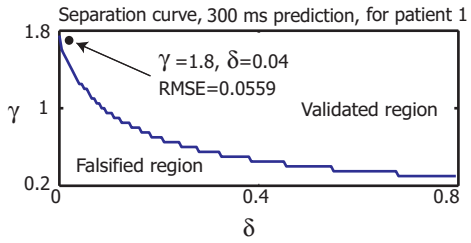

Figure 1: Separation curve for patient 1 for a 300 ms prediction

Table 1: Prediction performance, NRMSE $\times$ 100.

Prediction algorithm	Latency (ms)	Patient case number								
		1	2	3	4	5	6	7	8	9
NSM	100	23.56%	16.14	5.60	22.02	29.01	22.94	26.23	15.86	31.32
	200	27.01	19.70	5.96	25.38	36.65	27.80	34.69	19.32	32.92
	300	30.04	23.91	6.19	28.17	42.16	32.46	46.45	22.98	35.60
	400	32.27	26.73	6.37	30.67	47.65	36.54	53.14	26.56	39.66
	500	35.13	29.98	6.55	32.65	52.91	40.41	58.54	29.96	40.78
Optimized NN	100	13.73%	6.99	07.56	30.33	59.11	13.72	29.00	08.81	28.69
	200	25.41	10.86	19.12	50.22	151.2	28.76	49.00	14.40	43.78
	300	38.26	16.44	32.71	95.67	266.4	49.74	70.00	24.67	108.2
	400	51.68	21.78	46.25	131.3	283.3	76.59	70.00	34.06	156.8
	500	63.79	25.50	59.49	164.3	330.5	90.05	92.00	41.73	206.58
NN in [23]	100	32.00%	12.00	30.00	19.00	19.00	23.00	29.00	17.00	40.00
	200	50.00	18.00	50.00	32.00	37.00	35.00	49.00	27.00	65.00
	300	63.00	23.00	68.00	38.00	47.00	45.00	70.00	34.00	86.00
	500	92.00	32.00	84.00	66.00	61.00	62.00	92.00	50.00	100.0

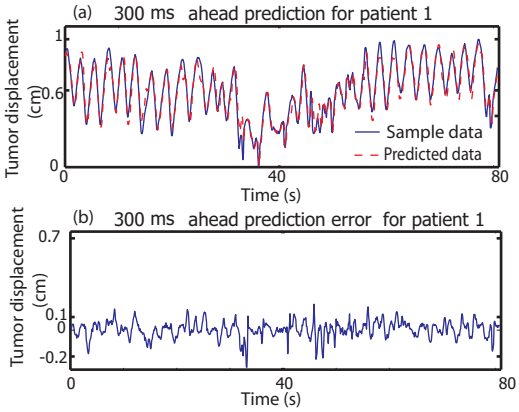

Figure 2: 300 ms prediction result for patient 1

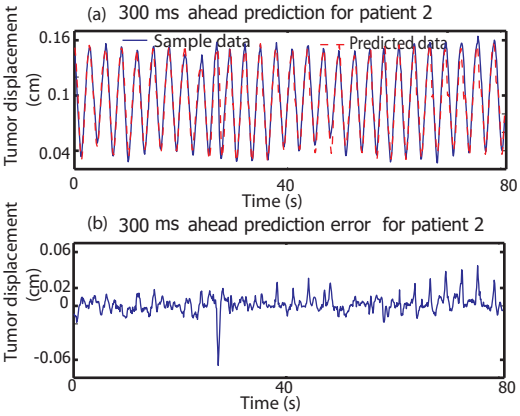

Figure 3: 300 ms prediction result for patient 2

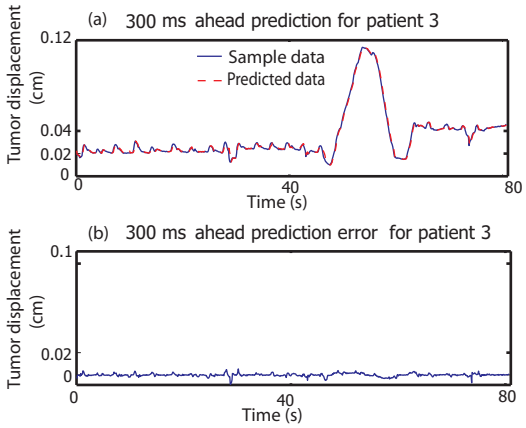

Figure 4: 300 ms prediction result for patient 3